Physica B 536 (2018) 833–838

Contents lists available at ScienceDirect

Physica B

journal homepage: www.elsevier.com/locate/physb

Upper critical and irreversibility fields in Ni- and Co-doped pnictide bulk superconductors

Martin Nikolo[a,*], John Singleton[b], Dmitry Solenov[a], Jianyi Jiang[c], Jeremy Weiss[c], Eric Hellstrom[c]

[a] Department of Physics, Saint Louis University, St. Louis, MO 63103, USA
[b] National High Magnetic Field Laboratory, Los Alamos National Laboratory, Los Alamos, NM 87545, USA
[c] Applied Superconductivity Center, National High Magnetic Field Laboratory, Florida State University, Tallahassee, FL 32310, USA

ARTICLE INFO

Keywords:
Superconductivity
Pnictides
Upper critical magnetic field
Irreversibility field

ABSTRACT

A comprehensive study of upper critical and irreversibility magnetic fields in $Ba(Fe_{0.95}Ni_{0.05})_2As_2$ (large grain and small grain samples), $Ba(Fe_{0.94}Ni_{0.06})_2As_2$, $Ba(Fe_{0.92}Co_{0.08})_2As_2$, and $Ba(Fe_{0.92}Co_{0.09})_2As_2$ polycrystalline bulk pnictide superconductors was made in pulsed fields of up to 65 T. The full magnetic field-temperature (*H-T*) phase diagrams, starting at 1.5 K, were measured. The higher temperature, upper critical field H_{c2} data are well described by the one-band Werthamer, Helfand, and Hohenberg (WHH) model. At low temperatures, the experimental data depart from the fitted WHH curves, suggesting an emergence of a new phase that could be attributed to the Fulde-Ferrell-Larkin-Ovchinnikov (FFLO) state. The large values of the Maki fitting parameter α indicate that the Zeeman pair breaking dominates over the orbital pair breaking and spin-paramagnetic pair-breaking effect is significant in these materials. Possible multi-band structure of these materials is lumped into effective parameters of the single-band model. Table of measured physical parameters allows us to compare these pnictide superconductors for different Co- and Ni- doping levels and granularity.

1. Introduction

The upper critical field, $\mu_0 H_{c2}$, is one of the fundamental parameters in type II superconductors and provides important insight into the Cooper-pair-breaking mechanisms in a magnetic field [1–3]. Since the Fe-based superconductors have large upper critical fields, there are not many facilities where high H_{c2}'s can be measured at low temperatures; attempts to extrapolate the higher temperature $H_{c2}(T)$'s to low temperatures usually overestimate the actual values [4,5]. Measurements in large (> 50 T) magnetic fields are therefore needed to understand the low temperature $H_{c2}(T)$ behavior [6].

There are two distinct ways to induce pair-breaking in type-II superconductors by an applied magnetic field – by orbital or spin paramagnetic effects [1]. The relative importance of the orbital and paramagnetic effects in the suppression of the superconductivity is described by the Maki parameter $\alpha = \sqrt{2}\, H_{c2}^{orb}/H_{c2}^{P}$ where α is of the order of Δ/ε_F, where Δ is the BCS energy gap function and ε_F is the Fermi energy [7]. In most superconductors, the Maki parameter is usually much less than unity and this indicates that the influence of the paramagnetic effect is negligibly small [7]. However, in materials with heavy electron effective mass, in which the Fermi energy is small, or in layered materials in a magnetic field parallel to the layers, α can be larger than unity [1–3].

In the present work, we apply 0–65 T magnetic fields to polycrystalline samples of Fe-based superconductors to assess which of the above mechanisms dominates their low-temperature performance. By fitting the temperature dependence of the upper critical field we derive descriptive constants such as the Maki parameter and assess how these vary with Co and Ni doping, as we search for clues as to possible future enhancements of these materials.

2. Methods

2.1. Fitting the temperature dependence of the upper critical field

Orbital effects on the temperature dependence of the upper critical field $H_{c2}(T)$ were first considered by Helfand and Werthamer (HW) [1]. Their methods have been used routinely to analyze data on new superconductors with strongly anisotropic Fermi surfaces and order parameters, despite the fact that HW considered only the isotropic s-wave spherical symmetry of the Cooper pair [1]. In a second paper, Werthamer, Helfand, and Hohenberg (WHH) added the effects of both

* Corresponding author.
E-mail address: nikolom@slu.edu (M. Nikolo).

http://dx.doi.org/10.1016/j.physb.2017.09.047
Received 29 June 2017; Received in revised form 16 August 2017; Accepted 13 September 2017
Available online 19 September 2017

Pauli paramagnetism and spin–orbital scattering to predict the universal behavior of the upper critical field $H_{c2}(T)$ in superconductors with weak electron-phonon coupling [1]. In the dirty limit, when the overall mean free time τ is much less then $1/T$ in units with $k_B = 1$, WHH demonstrated that the critical field is found by setting [1]

$$f(t, h; \alpha, \lambda_{so}) = \ln t + \sum_{n=-\infty}^{\infty} \left\{ \frac{1}{|2n+1|} - \left[|2n+1| + \frac{h}{t} + \frac{(\alpha h/t)^2}{|2n+1| + (h+\lambda_{so})/t} \right]^{-1} \right\} \quad (1)$$

to zero, i.e., $f(t, h; \alpha, \lambda_{so}) = 0$. The dimensionless parameters are defined as

$$t = T/T_c, \qquad h = eH_{c2}v_F^2\tau/3\pi T_c, \qquad \alpha = 3/2mv_F^2\tau, \qquad \lambda_{so} = 1/3\pi T_c\tau_{so}, \quad (2)$$

where v_F is the Fermi velocity and τ_{so} is the mean free time due to spin-orbit scattering; the parameter λ_{so} describes the strength of the spin–orbit scattering.

A number of workers have used the WHH formalism to fit their H_{c2}(T) data [8–11]. For FeTeSe and FeTeS single-crystal superconductors, the Maki parameters are larger than 1. For FeTeS good fits were obtained using the WHH parameters $\alpha \approx 3–4$ and $\lambda_{so} \approx 0.5–1$, while for FeTeSe the parameters were $\alpha \approx 4–5$ and $\lambda_{so} \approx 1$ [8–10]. In the WHH-one band scheme, the relative strength of the spin-paramagnetic effect over the orbital-limiting effect tells us that spin-paramagnetic pair-breaking effect is dominant.

In many pnictides, the situation is complicated by the mild anisotropy of the upper critical field [11] and other effects that lead to a variety of different temperature dependences. Ghannadzadeh et al. measured upper critical fields of NaFe1-xCoxAs single crystals in fields parallel and perpendicular to the ab planes [12]. The $H_{c2}(T)$ data were fitted to the WHH model. For fields parallel to the *ab* planes $H_{c2}(T)$ is well described by the WHH model across all temperatures. However, for field perpendicular to the *ab* planes, the WHH model fitted the data only close to T_c; at lower temperatures, the upper critical field grew at a faster rate. A similar effect was noted by Yuan et al. [13]; for *H* perpendicular to the ab planes, H_{c2} followed an almost linear increase with decreasing temperatures. Ghannadzadeh et al. [12] model their data via both one-band and two-band WHH models but also speculate that there exists the possibility of a Fulde-Ferrell-Larkin-Ovchinnikov (FFLO) phase.

The departure from the typical WHH convex $H_{c2}(T)$ curves has been attributed to two possible mechanisms. The upward curvature in $H_{c2}(T)$ for perpendicular fields is suggested to be due to the multiband nature of the superconductivity. This is thought to be the case for the rare-earth 1111 systems (ReFeAsO$_{1-x}$F$_x$ where *Re* is a rare-earth atom) [11,14,15], the 122 systems ($BaFe_2As_2$) [16], and the closely related 111 superconductor LiFeAs [14], amongst others. Comparison with measurements of MgB_2 suggest that pnictide superconductors have multiple bands contributing to superconductivity; [14,17] though in the case of the pnictides, the enhancement of H_{c2} over BCS expectations is significant. This large enhancement over the orbital pair breaking which limits $H_{c2}(T)$ in conventional superconductors indicates that pnictides may be close to the Fulde–Ferrell–Larkin–Ovchinnikov (FFLO) phase [18,19]. This has been suggested by several workers [12–14].

In the FFLO phase, the Zeeman splitting causes a nonzero momentum of the Cooper pairs, and spatial oscillations of the superconducting order parameter [18,19]. The orbital pair breaking effect must be weak relative to the Pauli paramagnetic effect. Materials with large effective electron masses or layered materials (with quasi-two-dimensional electrical conduction) are candidates for the FFLO state. Spatial modulation of the gap function of the form $c_1e^{i\mathbf{Qr}} + c_2e^{-i\mathbf{Qr}}$ offsets the transition to the normal (paramagnetic) state to higher magnetic fields [14,16]. Calculations show that in anisotropic superconductors the FFLO state might lead to an enhancement of the upper critical field H_{c2} to between 1.5 and 2.5 times the Pauli paramagnetic limit [20,21]. Evidence of the FFLO state has been found in heavy fermion [22–25] and organic [26–31] superconductors.

In polycrystalline samples such as ours – i.e. those that will be employed in technological applications – the anisotropy of the superconductivity seen in single crystals will nevertheless be manifested. Proximity effect arguments [32] suggest that whichever is the higher of the critical fields (parallel or perpendicular to the ab planes) at a particular temperature will dominate the behavior of polycrystals. Using the precedent of single-crystal measurements [12,13], we expect that the WHH fit will work well close to T_c, but that the emergence of any quasi-linear enhancement will take over at lower temperatures. Thus, in the analysis below, we develop and use the WHH model to fit data from our polycrystalline samples and make a qualitative assessment of the lower temperature linear deviation. The parameters extracted from WHH allow us to speculate whether the quasi-linear deviations at low temperatures are due to the FFLO state or not.

2.2. Experimental details

The Co-doped samples used in this study were $Ba(Fe_{0.92}Co_{0.08})_2As_2$ (Co8) (T_c = 23.2 K) and $Ba(Fe_{0.92}Co_{0.09})_2As_2$ (Co9) (T_c = 25.3 K) bulk, polycrystalline pnictide superconductors. The materials were cut into parallelepipeds with dimensions of 0.7 × 0.7 × 4.9 mm^3 and 0.6 × 0.7 × 2.0 mm^3, respectively. Also, we studied three different Ni-doped samples. We measured two $Ba(Fe_{0.95}Ni_{0.05})_2As_2$ (Ni5) polycrystalline superconductors. The average grain size of one was about 17 μm and its T_c was 19.2 K. The average grain size of the other was larger and its T_c was 20.4 K. We distinguish between those two Ni5 samples as follows: the larger grain and higher T_c sample is labelled Ni5(LG), and smaller grain and lower T_c sample is Ni5(SG). Ni5(LG) had very low grain connectivity, large grain size, and some FeAs impurities were observed between most grains. Third Ni-doped sample that we measured was a $Ba(Fe_{0.94}Ni_{0.06})_2As_2$ (Ni6) polycrystalline sample whose T_c was 18.5 K. The parallelepiped dimensions of the samples were: Ni5(LG) – 0.7 × 0.7 × 2 mm^3, Ni5(SG) – 0.6 × 0.75 × 3.9 mm^3, and Ni6 – 0.7 × 0.7 × 2 mm^3, respectively.

The samples were synthesized at the Applied Superconductor Center (at the National High Magnetic Field Laboratory) [33,34], Upper critical fields were measured in pulsed magnetic fields of up to 65 T at the National High Magnetic Field Laboratory (NHMFL) campus in Los Alamos, NM. A radio-frequency proximity detector oscillator (PDO) induction technique was used, in which the sample is placed inside a coil that forms part of a tank circuit whose resonance frequency is monitored as a function of field and temperature [33–36]. In a second part of the experiment, we measured the sample's magnetization in pulsed fields of up to 65 T, using a compensated, inductive extraction magnetometer probe [37] to determine the irreversibility fields.

3. Results and analysis

From the PDO frequency vs. magnetic field plots at multiple temperatures we determined the upper critical fields. Fig. 1(a)–(f) plots H_{c2} and H_{irr} fields as a function of temperature for Co8, Co9, Ni5(LG), Ni5(SG), and Ni6 samples. Our polycrystalline data show higher H_{c2}'s than results reported by another group on crystalline $Ba(Fe_{0.926}Co_{0.074})_2As_2$ (Co7.4), $Ba(Fe_{0.896}Co_{0.114})_2As_2$ (Co11.4), and $Ba(Fe_{0.954}Ni_{0.046})_2As_2$ (Ni4.6) samples, measured both parallel and perpendicular to the ab planes [38,39]. This confirms the high quality of the bulk samples prepared by the FSU group.

We do not get the concave downward plots seen in typical traditional type II superconductors [32,40]. Most of the data could

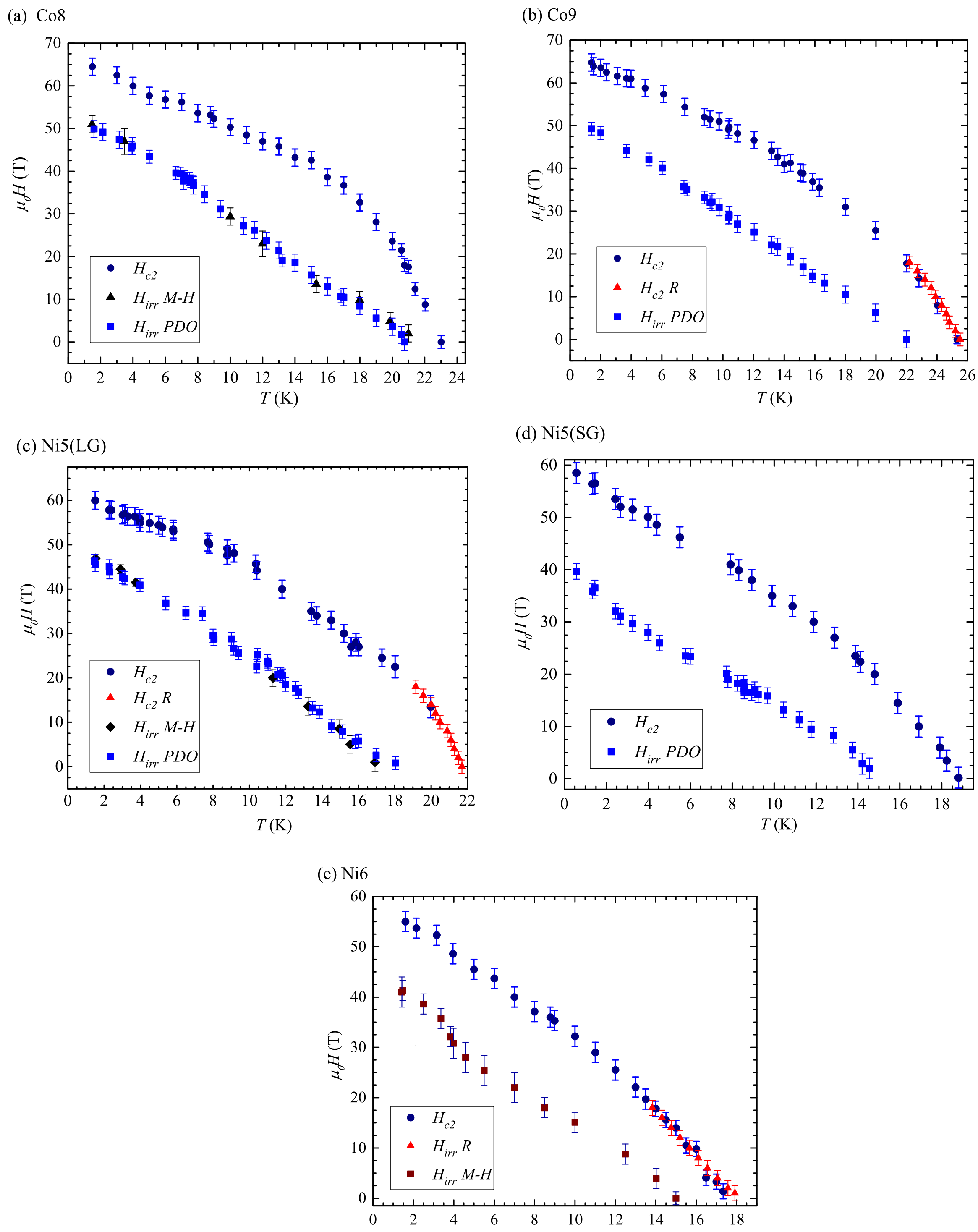

Fig. 1. H_{c2} and H_{irr} as a function of temperature for (a) Co8, (b) Co9, (c) Ni5(LG), (d) Ni5(LG), and (e)Ni6. H_{c2} is consistently linear near T_c and also appears linear in low temperatures. Data obtained from resistivity measurements are marked *R*, data from magnetization measurements are marked *M-H*, and H_{irr} data from PDO measurements are marked *PDO*.

be fitted by two different straight lines for each sample. We note the existence of a quite steep increase in the H_{c2} near T_c and the subsequent flattening of the curve at lower temperatures, although this flattening was very moderate for Ni5(SG) and Ni6 samples.

H_{c2}'s almost linear increase near T_c supports the presence of the multiband effect in the system [8]. In light of this, a more complete theoretical description of the H_{c2} curves in various iron pnictides is necessary so that it includes both the multiband orbital and Pauli paramagnetic effects simultaneously.

We observe a noticeable upturn in $H_{c2}(T)$ in low temperatures for the Co9 and Ni5(SG) samples. For the Ni5(SG), Ni5(LG), and Co9 samples we observe linear increase in H_{c2} with decreasing temperature at low temperatures. Several studies showed that $H_{c2}(T)$ exhibits quite a linear increase down to lowest temperatures in 122 compounds, not unlike our results [16,41,42].

Ni6 and Co8 samples show a little bit of H_{c2} flattening at lowest temperatures. Similar concave shape of $H_{c2}(T)$ curves was observed in 122, 111, and 11 pnictides (122 stands for $BaFe_2As_2$, 111 for AFeAs,

Table 1
Table of measured and derived critical parameters.

Sample	T_c (K)	H_{c2} at 1.5 K (T)	H_{irr} at 1.5 K (T)	$\frac{dH_{c2}}{dT}\vert_{T=T_c}$ (T/K)	$H_{c2}^{orb}(0)$ (T)	$H_{c2}^{P}(0)$ (T)	α	λ_{SO}	H_{c2}/H_{c2f} at 1.5 (K)	τ_{SO} (s)	H_{c2}/T_c (T/K)	t_{break}	ξ at 1.5 K (nm)
Co8	23.2	64.0	50.5	−8.8	140.9	42.7	6.5	0.9	1.08	$3.9\ 10^{-14}$	2.8	0.35	2.3
Co9	25.3	63.5	49.5	−6.3	110.0	46.6	4.4	0.5	1.28	$6.4\ 10^{-14}$	2.5	0.52	2.3
Ni5(SG)	19.2	57.5	37.5	−5.9	78.12	35.3	3.2	2.5	1.15	$1.7\ 10^{-14}$	3.0	0.29	2.4
Ni5(LG)	20.4	60.0	47.0	−7.1	99.9	37.5	3.2	2.0	1.06	$2.0\ 10^{-14}$	2.9	0.15	2.3
Ni6	18.5	55.0	41.0	−6.1	77.9	34.0	3.1	3.7	1.11	$1.2\ 10^{-14}$	3.0	0.28	2.4

where A is a metal such as Na, Li, etc., and 11 for $FeSe_{1-x}Te_x$) [8–10,15,16,43–48]. This $H_{c2}(T)$ flattening suggests strong Pauli limiting of H_{c2}, and indicates that these materials are candidates for the FFLO transition [1,7,18,19,49,50]. In the possible multi-band structure of these materials it is possible that FFLO could develop in only one of the bands.

Co8 has the steepest slope $dH_{c2}/dT = -8.8$ T/K at T_c among our samples (Table 1). This is one of the largest reported magnitudes for 122, iron-based superconductors [8–11]. This steepest slope at T_c also correlates with the highest measured H_{c2}(1.5 K) and H_{irr}(1.5 K) among our samples. The orbital-limiting field for a BCS superconductor with a single active band is determined by applying ${H_{c2}}^{orb}(0) = -0.693T_c(dH_{c2}/dT$ at $T = T_c)$ [1]. See Table 1. The calculated ${H_{c2}}^{orb}(0)$ values, as high as 140.9 T for Co8, are much larger than the observed values ranging between 55 and 64 T. This suggests that the low-temperature H_{c2} is predominantly a Pauli-limited upper critical field.

We calculate the expected Pauli-limiting field for a weakly coupled BCS superconductor, above which the pair-breaking Zeeman energy exceeds the binding energy of the Cooper pair, as ${H_{c2}}^{P}(0) = 1.84T_c$. It is much smaller than the predicted ${H_{c2}}^{orb}(0)$ as well as the experimental H_{c2}(1.5 K) (Table 1). This observation implies that the spin paramagnetic effect may play an important role in determining H_{c2} in this 122 system and that a mechanism to enhance the Pauli limiting field beyond the BCS theory might be necessary. The results are also consistent with calculations showing that in anisotropic superconductors the FFLO state might lead to an enhancement of the upper critical field H_{c2} to between 1.5 and 2.5 times the Pauli paramagnetic limit [20,21].

We note the relatively high H_{c2}'s compared to their T_c's. Table 1 shows that the H_{c2}/T_c ratio is as large as 3.0 for Ni5(SG) and Ni6. This is significantly higher than comparable ratios for bulk cuprates. The excellent H_{c2}/T_c properties make these bulk materials very promising for applications at liquid helium temperatures.

In order to examine the shape of the temperature dependence of the upper critical field we apply the WHH approach described earlier. We first notice that the sum over the Matsubara frequencies can be evaluated exactly leading to

$$f(t,\,h;\,\alpha,\,\lambda_{so}) = +\ln 4t + \frac{4\alpha^2h^2 - \lambda_{so}^2 - i\lambda_{so}\sqrt{4\alpha^2h^2 - \lambda_{so}^2}}{8\alpha^2h^2 - 2\lambda_{so}^2}\psi'([2h + \lambda_{so} + 2t - i\sqrt{4\alpha^2h^2 - \lambda_{so}^2}]/4t) + c.\,c. \tag{3}$$

where $\psi'(z) = d^2\ln\Gamma(z)/dz^2$ is the first derivative of the digamma function. Furthermore, near the zero-field critical point (and within the WHH assumptions) the function simplifies to

$$f(t \to 1,\, h \to 0;\, \alpha,\, \lambda_{so}) \to \frac{\pi^2}{4}h + (1 - t). \tag{4}$$

Introducing scattering-independent dimensionless field

$$h' \equiv \alpha h = eH_{c2}/2\pi T_c m \tag{5}$$

we notice that the Maki fitting parameter, α, is determined primarily by the high temperature data near the critical temperature, where

$$h' \approx 4\alpha\frac{1-t}{\pi^2}. \tag{6}$$

The spin-orbit scattering fitting parameter, λ_{so}, on the other hand, is primarily set by the lower temperature flattening region of the $h'(t)$ curve.

In Fig. 2(a)–(e) we plot dimensionless critical field h' as a function of $t = T/T_c$ while fitting the data for $f(t,\,h;\,\alpha,\,\lambda_{so}) = 0$. The fitting procedure results in $\alpha = 6.5$ and $\lambda_{so} = 0.9$ for Co8 (Fig. 2(a)), and $\alpha = 4.4$ and $\lambda_{so} = 0.5$ for Co9 (Fig. 2(b)) We also obtain $\alpha = 3.2$ and $\lambda_{so} = 2.0$ for Ni5(LG), $\alpha = 3.2$ and $\lambda_{so} = 2.5$ for Ni5(SG), and $\alpha = 3.1$ and $\lambda_{so} = 3.7$ for Ni6. Table 1 summarizes the results. The impact of different Maki and spin scattering parameters on the shape of the fitted curve and the structure of the WHH solution is discussed in our previous work [33].

The noticeable upturn in $H_{c2}(T)$ at low temperatures, especially for the Co9 sample, can not be explained via λ_{so} and α dependence of the $f(t,\,h;\,\alpha,\,\lambda_{so}) = 0$ curve if we assume the same homogeneous phase at all temperatures below T_c. These data suggest an emergence of a new phase. Gurevich [2,3] generalizes the WHH calculations to incorporate finite-Q FFLO state, and predicts a sudden increase of H_{c2} at low temperatures – the same linear upturn appears in our low temperature data. However multiple unknown parameters of that multi-band model makes fitting impractical in our case.

The higher temperature, upper critical field H_{c2} data is well described by the WHH model for all samples. Surprisingly, the one-band WHH model also describes the low temperature behavior of Ni5(LG) sample down to a $t = T/T_c$ of about 0.15 (Fig. 2). For the Ni5(SG) and Ni6 samples, the experimental data suddenly depart from the fitted WHH curve at a reduced temperature t of about 0.29 and 0.28. The Co8 and Co9 WHH fits depart from the measured data at $t = 0.35$ and $t = 0.52$, respectively. We determine the enhancement of our H_{c2} data relative to the WHH fitted H_{c2f} at T = 1.5 K by calculating H_{c2}/H_{c2f} and note that Co9 has the largest enhancement ratio of 1.28 while the other materials' enhancements relative to the WHH fit are near 1.1 and the one band fit is close to the measured values (Table 1).

The presence of the Maki parameter α describing the Pauli-limiting effect in the WHH scheme is essential to describe much smaller $H_{c2}(0)$ values than is expected for the orbital-limiting field. The large value of α indicates that the Zeeman pair breaking dominates over the orbital pair breaking and spin-paramagnetic pair-breaking effect is significant. Furthermore, the large value of $\alpha = 6.5$ for Co8 is comparable to that for CeCoIn5 and organic superconductors that have shown the first-order transition in H_{c2}, forming a Fulde-Ferrell-Larkin-Ovchinnikov FFLO-like state [51,52].

The obtained spin orbit scattering constants indicate that spin-orbit

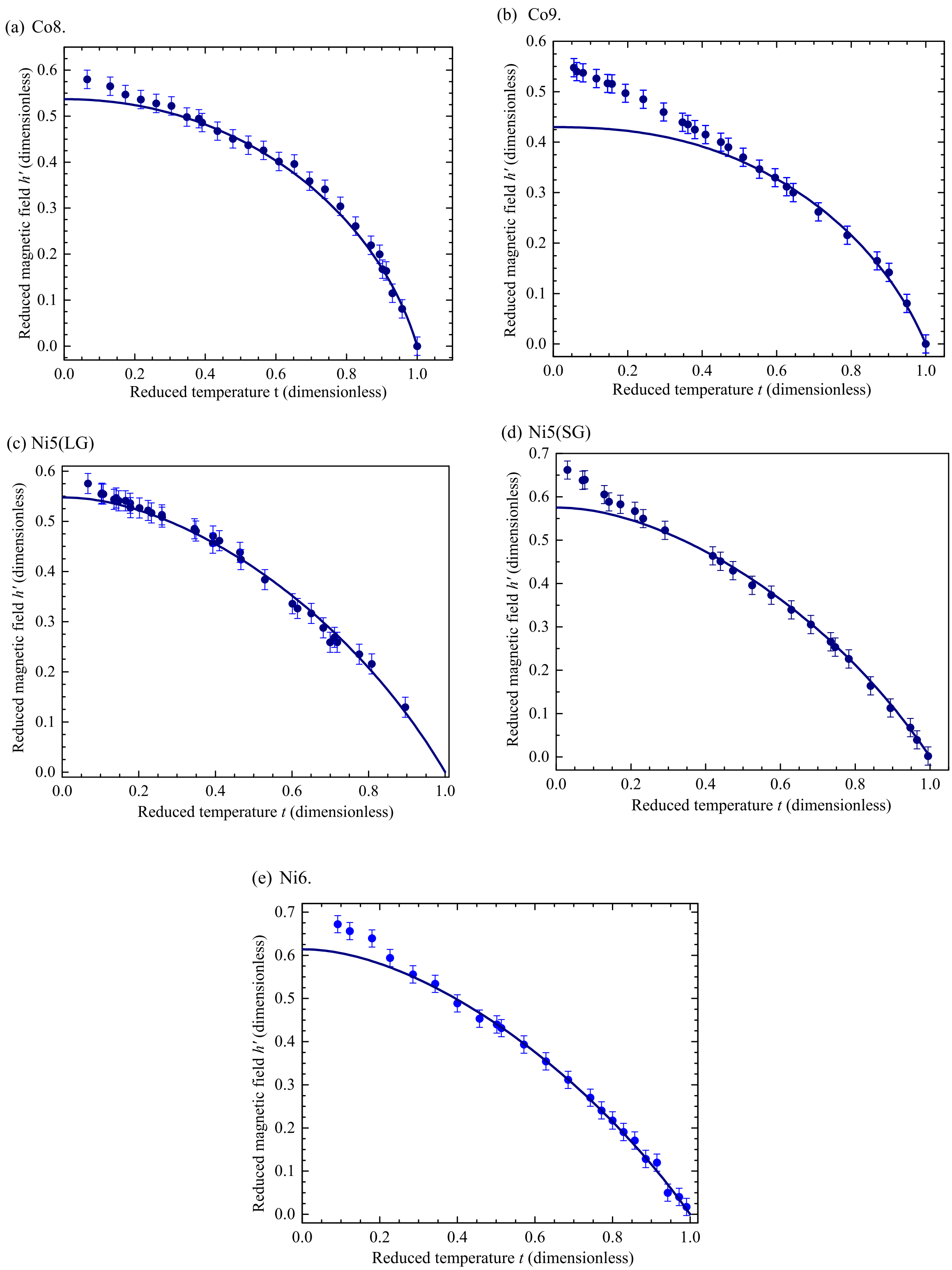

Fig. 2. WHH fit of reduced magnetic field h' versus reduced temperature t for (a) Co8, using α = 6.5 and λ = 0.9, (b) Co9, using α = 4.4 and λ = 0.5, (c) Ni5(LG), using α = 3.2 and λ = 2.0, (d) Ni5(SG), using α = 3.2 and λ = 2.5, and (e) Ni6, using α = 3.1 and λ = 3.7.

scattering needs to be included in describing the $H_{c2}(T)$ data. In the Co-doped pnictides, starting from the parent compound, λ_{so} decreases upon doping (Co8), due to the reduction in scattering from magnetic excitations as the system moves away from the long-range ordered AFM phase; λ_{so} then reaches a minimum at optimal doping (Co9), and begins to increase in the over doped region, possibly due to scattering from magnetic Co impurities [4]. This is consistent with the Ni5/Ni6 data as well where Ni6, or over doped sample, has higher λ_{so} relative to that of Ni5 which is optimally doped.

The spin orbit scattering constant $\lambda_{so} = h_{bar}/(3\pi k_B T_c \tau_{so})$ accounts for the spin-orbit and spin-flip scattering with τ_{so} as the mean free scattering time [12]. We determine τ_{so} for each sample. It ranges from 1.2 10^{-14} s for Ni6 (lowest T_c) to 6.4 10^{-14} s for Co9 (highest T_c). Measurement of $H_{c2}(T)$ also allows us to find the coherence length $\zeta(T)$

= $\sqrt{\phi_0/2\pi H_{c2}(T)}$ = 2.3 nm at T = 1.5 K for Co8, Co9, and Ni5(LG), and 2.4 nm for Ni5(SG) and Ni6, respectively (Table 1).

4. Conclusion

Radio frequency proximity detector oscillator induction technique in pulsed fields up to 65 T was applied to measure the temperature dependence of upper critical and irreversible magnetic fields of $Ba(Fe_{0.92}Co_{0.08})_2As_2$, $Ba(Fe_{0.91}Co_{0.09})_2As_2$, $Ba(Fe_{0.95}Ni_{0.05})_2As_2$ (LG) and (SG), and $Ba(Fe_{0.94}Ni_{0.06})_2As_2$ polycrystalline bulk pnictide superconductors. These measurements allow us to determine a range of physical parameters for each superconductor and compare them for different Co- and Ni- doping and granularity. Our polycrystalline samples were of high quality as they showed at least as high, and higher H_{c2}'s, than comparable data on single crystals by other groups. This shows suitability of the pnictide bulk materials for magnet design.

The temperature dependence of the upper critical field H_{c2} is of interest here. Our H_{c2} data is well described by the WHH model for all samples. A linear increase in H_{c2} with decreasing temperature is observed at low temperatures as the data departs from the fitted WHH curve in low temperatures, suggesting an emergence of a new phase that can be attributed to the FFLO state. The obtained values of Maki parameter indicate that the Zeeman pair breaking dominates over the orbital pair breaking and spin-paramagnetic pair-breaking effect is significant. The fitted spin orbit scattering constants indicate that spin-orbit scattering needs to be included in any model describing the $H_{c2}(T)$ behavior in these pnictide superconductors.

Both, the higher temperature behavior, as well as the low temperature curve, can be potentially described within a single-band model WHH with added finite-Q dependence (Q is a wave vector of FFLO oscillations) to introduce FFLO state as described by Gurevich [2,3]. In this case, possible multi-band structure of these materials could be lumped into effective parameters of the single-band model. However, if FFLO develops in only one of the bands, the expanded influence on the form of H_{c2} is lesser and the upturn in the H_{c2} data in low temperatures is smaller, possibly the case of the $Ba(Fe_{0.92}Co_{0.08})_2As_2$ sample. Anisotropy in the behavior of the upper critical field also plays a role in the explanation of the data, as we see some kind of H_{c2} averaging of different granular orientations. In light of this, a more complete theoretical description of the H_{c2} curves in various iron pnictides is necessary so that it includes both the multiband orbital and Pauli paramagnetic effects simultaneously and at the same time is not dependent on too many fitting constants that cannot be accessed by experiment.

Acknowledgements

A portion of this work was performed at the National High Magnetic Field Laboratory, which is supported by National Science Foundation Cooperative Agreement No. DMR-1157490, the Department of Energy and the State of Florida.

References

[1] (a) E. Helfand, N.R. Werthamer, Phys. Rev. 147 (1966) 288;
(b) N.R. Werthamer, E. Helfand, P.C. Hohenberg, Phys. Rev. 147 (1966) 295.
[2] A. Gurevich, Phys. Rev. B 82 (2010) 184504.
[3] A. Gurevich, Phys. Rev. B 67 (2003) 184515 Physica C, 456, 160 (2007).
[4] M. Nikolo, X. Shi, J. Jiang, J.D. Weiss, E.E. Hellstrom, J. Supercond. Nov. Magn. 27 (9) (2014) 1983–1990.
[5] M. Nikolo, X. Shi, J. Jiang, J.D. Weiss, E.E. Hellstrom, J. Supercond. Nov. Magn. 27 (10) (2014) 2231–2239.
[6] J. Zhang, et al., Front. Phys. 6 (4) (2011) 463–473.
[7] K. Maki, Phys. Rev. 148 (1966) 362–369.
[8] S. Khim, J.W. Kim, E.S. Choi, Y. Bang, M. Nohara, H. Takagi, K.H. Kim, Phys. Rev. B 81 (2010) 184511.
[9] H. Lei, R. Hu, E.S. Choi, J.B. Warren, C. Petrovic, Phys. Rev. B 81 (2010) 094518.
[10] H. Lei, Rongwei Hu, E.S. Choi, J.B. Warren, C. Petrovic, Phys. Rev. B 81 (2010) 184522.
[11] H.-S. Lee, M. Bartkowiak, J.-H. Park, J.-Y. Lee, J.-Y. Kim, N.-H. Sung, B.K. Cho, C.-U. Jung, J.S. Kim, H.-J. Lee, Phys. Rev. B 80 (2009) 144512.
[12] S. Ghannadzadeh, et al., Phys. Rev. B 89 (2014) 054502.
[13] H.Q. Yuan, J. Singleton, F.F. Balakirev, S.A. Baily, G.F. Chen, J.L. Luo, N.L. Wang, Nature 457 (2009) 565.
[14] K. Cho, H. Kim, M.A. Tanatar, Y.J. Song, Y.S. Kwon, W.A. Coniglio, C.C. Agosta, A. Gurevich, R. Prozorov, Phys. Rev. B 83 (2011) 060502(R).
[15] J. Jaroszynski, F. Hunte, L. Balicas, Y.-j. Jo, I. Raiˇcevi´c, A. Gurevich, D.C. Larbalestier, F.F. Balakirev, L. Fang, P. Cheng, Y. Jia, H.H. Wen, Phys. Rev. B 78 (2008) 174523.
[16] M. Kano, Y. Kohama, D. Graf, F. Balakirev, A.S. Sefat, M.A. McGuire, B.C. Sales, D. Mandrus, S.W. Tozer, J. Phys. Soc. Jpn. 78 (2009) 084719.
[17] V. Braccini, et al., Phys. Rev. B 71 (2005) 012504.
[18] P. Fulde, R.A. Ferrel, Phys. Rev. 135 (1964) A550–A563.
[19] A.I. Larkin, Yu.N. Ovchinnikov, Zh. Exp. Teor. Fiz. 47 (1964) 1136–1146 Engl. Transl. Sov. Phys.–JETP, 20, 762 (1965).
[20] (a) H. Shimahara, J. Phys. Soc. Jpn. 66 (1997) 541;
(b) H. Shimahara, J. Phys. Soc. Jpn. 67 (1998) 1872.
[21] A.I. Buzdin, V.V. Tugushev, Zh. Eksp. Teor. Fiz. 85 (1983) 735 Engl. Transl. Sov. Phys.–JETP, 85, 428 (1983).
[22] A. Bianchi, R. Movshovich, C. Capan, P.G. Pagliuso, J.L. Sarrao, Phys. Rev. Lett. 91 (2003) 187004.
[23] M. Radovan, N.A. Fortune, T.P. Murphy, S.T. Hannahs, E.C. Palm, S.W. Tozer, D. Hall, Nat. Lond. 425 (2003) 51.
[24] K. Kumagai, K. Kakuyangi, M. Saitoh, S. Takashima, M. Nohara, H. Takagi, Y. Matsuda, J. Supercond. Nov. Magn. 19 (2006) 1.
[25] M. Kenzelmann, Th Strässle, C. Niedermayer, M. Sigrist, B. Padmanabham, M. Zolliker, A.D. Bianchi, R. Movshovich, E.D. Bauer, J.L. Sarrao, J.D. Thompson, Science 321 (2008) 1652.
[26] J. Singleton, J.A. Symington, M.S. Nam, A. Ardavan, M. Kurmoo, P. Day, J. Phys. Condens. Matter 12 (2000) L641–L648.
[27] S. Uji, T. Terashima, M. Nishimura, Y. Takahide, T. Konoike, K. Enomoto, H. Cui, H. Kobayashi, A. Kobayashi, H. Tanaka, M. Tokumoto, E.S. Choi, T. Tokumoto, D. Graf, J.S. Brooks, Phys. Rev. Lett. 97 (2006) 157001.
[28] R. Lortz, Y. Wang, A. Demuer, P.H.M. Böttger, B. Bergk, G. Zwicknagl, Y. Nakazawa, J. Wosnitza, Phys. Rev. Lett. 99 (2007) 187002.
[29] S. Yonezawa, S. Kusaba, Y. Maeno, P. Auban-Senzier, C. Pasquier, K. Bechgaard, D. Jerome, Phys. Rev. Lett. 100 (2008) 117002 J. Phys. Soc. Jpn., 77, 054712 (2008).
[30] M.A. Tanatar, T. Ishiguro, H. Tanaka, H. Kobayashi, Phys. Rev. B 66 (2002) 134503.
[31] C.C. Agosta, N.A. Fortune, S.T. Hannahs, S. Gu, L. Liang, J.-H. Park, J.A. Schleuter, Phys. Rev. Lett. 118 (2017) 267001.
[32] J. Annette, Superconductivity, Superfluids, and Condensates (Oxford Master Series in Condensed Matter Physics), 1 ed., Oxford University Press, Oxford, 2004.
[33] M. Nikolo, J. Singleton, D. Solenov, J. Jiang, J.D. Weiss, E.E. Hellstrom, J. Supercond. Nov. Magn. 30 (2017) 331–341.
[34] M. Nikolo, J. Singleton, D. Solenov, J. Jiang, J.D. Weiss, E.E. Hellstrom, J. Supercond. Nov. Magn. 30 (2017) 561–568.
[35] M.M. Altarawneh, C.H. Mielke, J.S. Brooks, Rev. Sci. Instrum. 80 (2009) 066104.
[36] S. Ghannadzadeh, et al., Rev. Sci. Instrum. 82 (2011) 113902.
[37] P.A. Goddard, et al., New J. Phys. 10 (2008) 083025.
[38] N. Ni, M.E. Tillman, J.-Q. Yan, A. Kracher, S.T. Hannahs, S.L. Bud'ko, P.C. Canfield, Phys. Rev. B 78 (2008) 214515.
[39] N. Ni, A. Thaler, J.Q. Yan, A. Kracher, E. Colombier, S.L. Bud'ko, P.C. Canfield, Phys. Rev. B 82 (2010) 024519.
[40] M. Tinkham, Introduction to superconductivity, Courier (2004) 134–135.
[41] S.A. Baily, Y. Kohama, H. Hiramatsu, B. Maiorov, F.F. Balakirev, M. Hirano, H. Hosono, Phys. Rev. Lett. 102 (2009) 117004.
[42] S. Khim, J.S. Kim, J.W. Kim, S.H. Lee, F.F. Balakirev, Y. Bang, K.H. Kim, Physica C 470 (2010) S317.
[43] A. Yamamoto, L. Balicas, J. Jaroszynski, C. Tarantini, J. Jiang, A. Gurevich, D.C. Larbalestier, R. Jin, A.S. Sefat, M.A. McGuire, B.C. Sales, D.K. Christen, D. Mandrus, Appl. Phys. Lett. 94 (2009) 062511.
[44] T. Kida, T. Matsunaga, M. Hagiwara, Y. Mizuguchi, Y. Takano, K. Kindo, J. Phys. Soc. Jpn. 78 (2009) 113701.
[45] T. Terashima, M. Kimata, H. Satsukawa, A. Harada, K. Hazama, S. Uji, H. Harima, G.-F. Chen, J.-L. Lio, N.-L. Wang, J. Phys. Soc. Jpn. 78 (2009) 063702.
[46] D. Braithwaite, G. Lapertot, W. Knapo, I. Sheikin, J. Phys. Soc. Jpn. 79 (2010) 053703.
[47] M. Fang, J. Yang, F.F. Balakirev, Y. Kohama, J. Singleton, B. Qian, Z.Q. Mao, H. Wang, H.Q. Yuan, Phys. Rev. B 81 (2010) 020509 R.
[48] M. Takahashi, T. Mizushima, K. Machida, Phys. Rev. B 89 (2014) 064505.
[49] G. Sarma, J. Phys. Chem. Solids 24 (1963) 1029.
[50] L.W. Grunberg, L. Gunther, Phys. Rev. Lett. 16 (1966) 996.
[51] I.J. Lee, M.J. Naughton, G.M. Danner, P.M. Chaikin, Phys. Rev. Lett. 78 (1997) 3555.
[52] H.A. Radovan, N.A. Fortune, T.P. Murphy, S.T. Hannahs, E.C. Palm, S.W. Tozer, D. Hall, Nature 425 (2003) 51.